Invited Paper

Terahertz *in-vivo* studies: improving experimental techniques to eliminate variables

Rayko Ivanov Stantchev [1], Qiushuo Sun [1], Shuting Fan [2], Xuequan Chen [1], and Emma Pickwell-MacPherson [1, 3*]
[1] Department of Electronic Engineering, The Chinese University of Hong Kong, Shatin, Hong Kong
[2] College of Electronic Science and Technology, Shenzhen University, 3688 Nanhai Rd, Shenzhen, Guangdong, China 518060
[3] Department of Physics, Warwick University, Coventry, UK
[*] Email: e.pickwell.97@cantab.net

(Recived Auguest 31, 2018)

Abstract: THz spectroscopic imaging is highly sensitive to water content, and as abnormal water content is usually indicative of afflictions THz imaging has great medical potential in early-stage disease diagnosis. However, clinical use requires fast acquisition, repeatability and cost-effective, reliable equipment, which is not yet offered by THz technology. In this work we have reviewed the methods and technologies that have the potential of allowing the transference of THz from the laboratory to the hospital. First, we discuss the need for reliable sample characterization and the calibration methods that overcome the relevant problems. Second, we discuss the usefulness of THz in disease diagnosis and further outline how occlusion of the skin must be accounted for accurate diagnosis. Thirdly, we discuss how adaptive sampling and smart image under-sampling can be used to reduce measurement times.

Keywords: Terahertz spectroscopy, Dermatology, Terahertz imaging, Adaptive imaging, THz modulation, Compressed sensing, Scar healing.

doi: 10.11906/TST.001-011.2019.03.01

1. Introduction

Water is fundamental to all biological life, thus abnormal water content is usually associated with disease and afflictions. Therefore, accurate measurement of water concentration in biological samples is of great importance. THz-spectroscopy is highly sensitive to water content [1] and thus has great potential for early disease diagnosis. Combined with the non-ionizing photon energies and non-invasive measurement nature of THz radiation, there has been a great effort to develop THz imaging for clinical use [2-7]. For example, it has been shown that THz imaging can observe human scar healing [2], diabetic foot syndrome [3], water content of the eye [4, 5], burn wounds [6] and dysplasia [7]. There is even the potential of using doing such imaging in the near-field for improved resolution [8].

Despite such potential THz is still far from being widely used in the hospitals and there have

been very few THz *in vivo* studies as measurements currently require complicated calibration algorithms [5, 9-12]. A common calibration method usually used for *in-vivo* skin imaging places the skin area of interest in direct contact with a quartz imaging window. This then allows one to simply remove the sample and use the resulting signal as a reference for the post-processing necessary in determining the sample properties (extracting the water content). However, contact with the quartz window has two major effects: occlusion and mechanical deformation of the subject's skin. The mechanism of occlusion influencing *in-vivo* THz spectroscopy has been investigated [13] and exploited to determine water diffusivity [14], however, the effect of mechanical deformation on the target's skin caused by an unevenly applied pressure is not well understood. Clarys *et al.* reported that the local hydration capacitance of skin increases with increasing pressure [15]. Their result indicated that pressure is a factor that cannot be ignored in the THz measurement of skin. These two problems need to be understood and eliminated as best as possible. The occlusion effect, the building up of water in the outermost skin layer, is exacerbated with prolonged contact with the quartz imaging window. Furthermore, patients can only remain still for short periods of time, hence the great need for faster acquisition speeds. The effect of applying pressure on the skin on the THz response has not been extensively studied hitherto and will be discussed in our future work.

In this paper, in section 2 we describe the calibration methods necessary to obtain reliable characterization of the sample's properties. Without these methods, extracting the water concentration becomes unreliable and hence accurate diagnosis is impossible. In section 3 we outline how THz can be used in the monitoring of scar-healing, and then discuss how the THz signals are affected by the skin coming into contact with a quartz imaging window for prolonged periods of time. Next in section 4, we describe experimental devices that have potential of improving the THz imaging acquisition rate as well as decreasing device costs. These include adaptive sampling of the THz waveform [16], compressed sensing of THz imaging [17-21] and THz modulators in a total internal reflection geometry [22, 23].

2. Accurate referencing

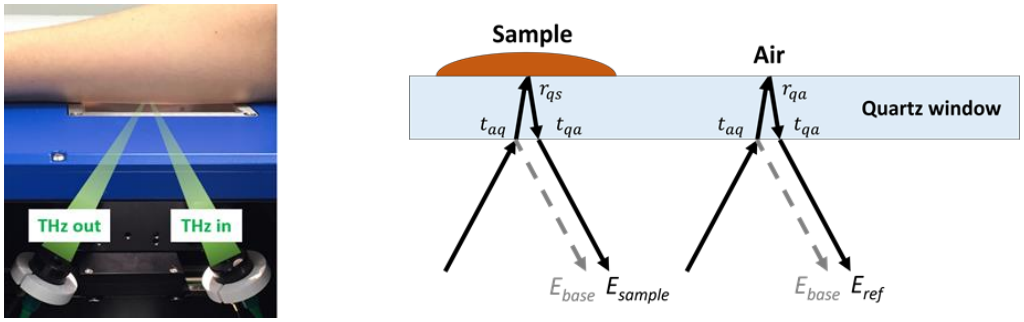

Fig. 1 *Left*: THz spectrometer setup for imaging human skin (volar forearm). *Right*: Detected sample and reference signals in a window-based reflection measurement.

In vivo measurements are desirable for real-time diagnosis, and as water has high absorption in the THz regime *in-vivo* monitoring, THz *in vivo* imaging can only be achieved with reflection type measurements. However, the human body is not very flat and hence can cause anomalies in the reflected THz signals. This is overcome by placing the sample, the subject's skin, onto a THz transparent imaging window (for example water-free quartz) as shown in figure 1 on the left. An emitter sends a THz pulse onto a quartz window with a subject's skin onto the skin in contact with the top surface of the quartz window, then a detector collects the reflected radiation. Note that THz spectrometers measure both the amplitude and phase of the detected signal [24], hence one can use Fresnel's reflection coefficients to obtain the complex refractive index of the sample. For this, one requires a suitable reference, ie. to measure the signal from a material whose refractive index is known. This is usually obtained by removing the sample and measuring the air signal as shown in figure 1 on the right. Since we know the refractive index of air (assumed to be 1), one can divide the measured signals by the reference signals, in the frequency domain, and equate them to the relevant Fresnel's coefficients to obtain an equation which can solved for the refractive index of the sample (see ref. [24] for details).

THz spectrometers measure the amplitude and phase information enabling the complex permittivity to be obtained. However, this capability also increases the potential sources of error. For example, amplitude fluctuations can be caused by jitter of optical delay stages, pump laser power instabilities and deterioration of the THz devices. Further, phase errors can be caused by optical fiber drift, mechanical positioning of the sample/reference and uneven window thickness. Figure 2 shows how some of these errors manifest themselves in measurements. Part **(a)** shows a typical reference signal, along with how it has changed after 6 hours. One can see two pulses at ~20*ps* and ~60*ps*. The first (second) pulse arises from the bottom (top) interface of the quartz window, as shown in the inset. The change in reference signal is mostly likely due to the THz

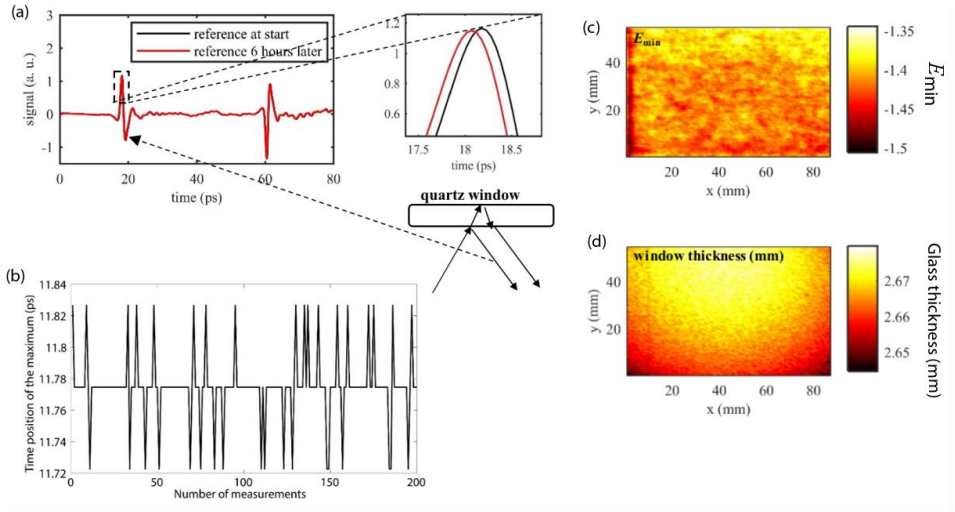

Fig. 2 (a) Reference measurement of air and 6hrs later. (b) Time position of the baseline maximum in 200 measurements (c) The THz field minimum value of a reflected signal over from a quartz; (d) Image of the window thickness calculated by the time delay between the reflections from bottom and upper surface and the refractive index of the window material.

devices and electronics reaching an equilibrium state. Further, there is a "ringing" signal after the first pulse, which can cause inaccuracies in the characterization of samples. Part (b) shows how jitter of the optical delay line affects the temporal position of the THz peak in 200 measurements. It can be seen that the THz peak temporal position can shift by up to 0.1*ps*, which affects the phase of the detected signal resulting in a characterization error [10]. Part (c) shows the minimum THz field value when imaging an empty quartz window – there is random variation in the image. Quartz has minimal THz absorption hence random thickness variation would not explain the resultant field values (and we can see from fig 2d that the thickness variation is not random). As the data was collected one-by-one in an *x-y* raster scanner, these random amplitude fluctuations arise from the power fluctuations of the laser powering the THz-spectrometer. Part **(d)** shows an image of the thickness of a quartz imaging window as calculated from the optical delay between the two pulses resultant from the top and bottom interfaces of the quartz window. It can be seen the quartz window has a thickness variation of ~30 μm, a length easily measurable by THz spectrometers.

The problems outlined above need to be eradicated for reliable sample characterization, and this can be accomplished with suitable reference measurements and post-processing as shown in the remainder of this section. The first work to be outlined here is that of Huang *et al* in ref. [12]. Therein the authors focused on removing any "ringing" artifacts in the signals caused by the reflection from the first window interface. Their method measures the signal when water is placed on to the quartz window, then simulate the signal they expect as the refractive index of water at THz frequencies has been widely studied [25-27]. The difference between the simulated and measured signal is their so called baseline signal which contains only the ringing artifacts from the first pulse. Subtraction of this baseline signal does improve the accuracy of their characterization results. However, their method is not primarily designed for imaging applications.

The first extension towards imaging was performed by Fan *et al* in ref. [9]. Therein the authors measured the free-space response of the quartz imaging window at every imaging point and afterwards the authors measured the quartz imaging window with water on top. This measurement allowed them to more accurately calculate the air-reference pulse resultant from the top-window interface, where the sample is placed, which allowed them to obtain a better sample characterization result. Their results (see ref. [9]) when measuring a 20% isopropanol-water show that their proposed method improves the standard deviation of the obtained refractive index (absorption coefficient) from 0.03 (1.77) to 0.006 (0.55). The reason for the improvement is that the calculation of their signals takes into account power fluctuations of the THz source (see fig. 2(**c**)). The benefits of their algorithm is that since the quartz imaging window is not changed on different days and hence the thickness at each imagining point remains the same, this calibration needs to be performed only once. To take into account the day-to-day power fluctuations and fiber-drift of the system, the authors measure a reference signal at a single-point. that. This reduces the total measurement time as the initial calibration of the reference signals can be calculated from the single-point measurement instead of re-measuring the reference at every point. Finally, the authors show that their algorithm has more consistent results when measuring the sample on different days.

However, to accurately account for the fiber-drift errors one needs to measure a few averages and one also needs to perform the measurement of a water-reference in addition to an air-reference.

Chen *et al* proposed a calibration algorithm achieving similar accuracy without needing the second water-reference at every image pixel and accounting for the fiber-drift error without simply averaging it out with many measurements in ref. [10]. Therein the authors measured the optical delay between the max values of the THz pulses across the entire imaging window, then they introduce a 2D interpolation fitting method called locally weighted scatterplot smoothing (LOWESS) fit. Around each data point, it fits a first-degree polynomial within a span with a distance weight assigned to all point within the span with closer points having a greater weight. Their result can be seen in figure 4(**b**), which gives a very smooth surface as the optical delay induced by the imaging window is calculated at each pixel. This smoothing fit has eliminated fluctuations and delay line jitters in a similar way to averaging out a few measurement sets whilst only requiring a single measurement at each point. Further, these signals have information about the laser-power status. Namely, the amplitude of the lower reflection is present in this air-reference measurement, thus one can normalize the amplitude of all the signals relative to a central position. Then after this calibration, from a single measurement at the central position one can calculate the relative reference signals, since the quartz window has not changed, as well as taking into account the current power of the laser and/or device performance. Finally, it needs to be pointed that Chen *et al* calculate the baseline signal for every image pixel from a single water-on-quartz window measurement at the central reference position. The authors then compare their algorithm to two traditional reference approaches: using the central point as a reference for all image pixels (named single reference) and measuring the signals from over the imaging area (named area reference). Their results can be seen in figures 4**(c-e)** with results from the single reference, area reference and

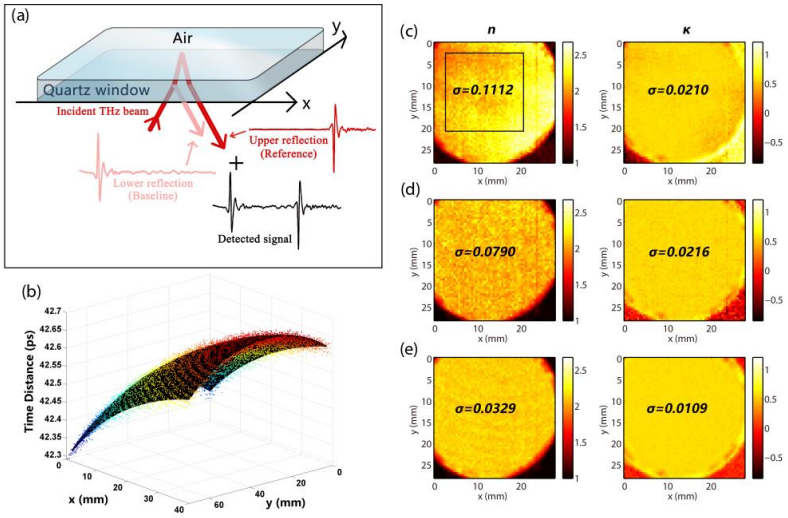

Fig. 4 (a) Illustration of the reflection system and examples of measured signals. (b) Time distance between the baseline and reference. The colorful points are the detected values. The black surface is acquired by LOWESS fitting. (c-e) The refractive index (*left*) and the absorption coefficient (*right*) image of water at 1THz, together with their standard deviation σ of the selected region, calculated by the (c) single approach, (d) area reference approach and (d) the proposed algorithm. Adapted from ref. [10].

the proposed algorithm shown respectively in parts **(c)**, **(d)** and **(e)**. It can be seen that the proposed algorithm performs best as it takes into account the thickness variation of the imaging window, not accounted for in the single reference, and also reduces effects from laser power fluctuations, which are not dealt with in the area reference technique.

3. Scar healing and water occlusion

The method developed in ref. [9] was used to monitor scar healing with THz radiation [2]. Figure 5 shows THz images of the refractive index and absorption coefficient along side optical images of the same scar. The image sets are taken 3, 5 and 6 months after injury going from top to bottom. In the 3-month images, parts **(a-c)**, the healthy tissue has much higher absorption corresponding to increased hydration levels compared the damaged area. Then the absorption of the scar increases during the healing process. When the skin is damaged it losses its barrier function, thus water escapes from the scar at an increased rate. Then as the skin heals it improves its barrier function and hence increasing the water content within the scar. The next obvious feature is the contrast in the refractive index for all time after injury. The authors speculate that this is due to damage to the collagen fibres that constitute the skin's non-water components. Damaged collagen fibres in scar tissues are known to be aligned in a more parallel manner when compared to normal tissue [28], and in the THz regime Lee *et al* reported differently aligned collagen fibres have different polarization-dependent properties [29]. Meanwhile, the Hendry group thereafter independently reported that articular cartilage, a bio-sample made mostly of collagen fibrils and water, has different THz properties depending on the incident polarization on a sub-THz wavelength scale [8]. Such studies indicate that THz can provide much information about the orientation and disorder of collagen fibrils during wound healing and in healthy/diseased tissue.

Whilst THz has many potential uses, the above measurements are still slow, requiring long acquisition times and as the skin has to be in contact with a quartz window there is another effect that need be considered. Namely, water occlusion in the skin's outer most layer as shown in by Sun

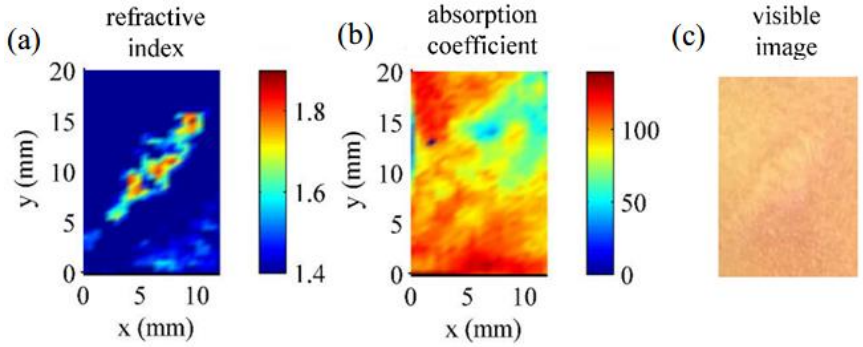

Fig. 5 THz images of the refractive index (a) and absorption coefficient (b) in comparison with the visible image for six months post-injury. Figure adapted from ref. [2]

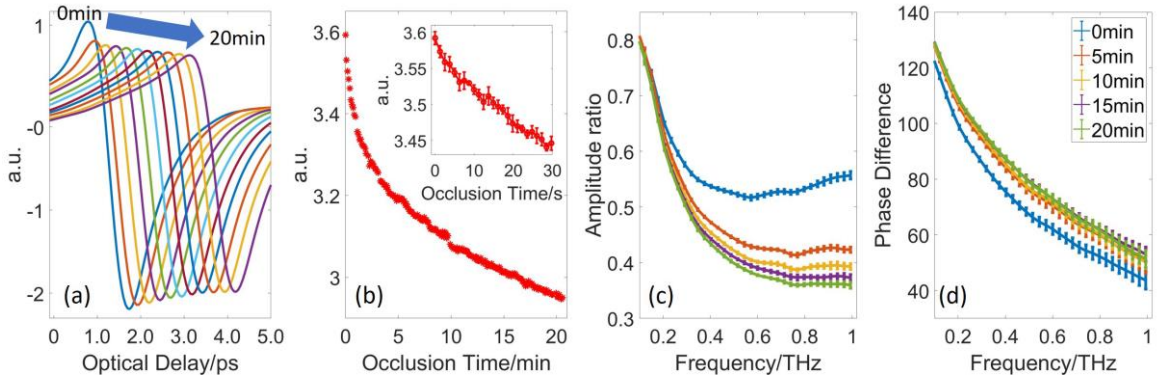

Fig. 6 (a) Processed THz signal with different occlusion times. The pulses have been shifted for clarity (b) The peak-to-peak of the processed THz signals occlusion time. Inset shows the peak-to-peak value in the first 30 seconds. (c-d) The spectrum of the amplitude ratio **(c)** and phase difference (d) between the sample and reference at 5 minutes intervals during 20 minutes of occlusion. From ref. [13].

et al in ref. [13]. Their results are shown in figure 6. In part **(a)** one can see the detected THz waveforms after the skin has been in contact with the imaging window for 0 up to 20 minutes in 2-minute intervals. It is obvious that the THz peak value decreases with time. In fig. 5**(b)** one can see the peak-to-peak value (maximum minus the minimum field value) as a function of occlusion time. Further, the inset shows that even 15 seconds of contact with the imaging window has an effect on the THz waveform. Parts **(c)** and **(d)** show the amplitude ratio and phase difference, respectively, between the skin and the reference signals in the frequency domain for different contact times with the window. The quantities in parts **(c-d)** are used in extracting the THz permittivity and inferring the content. Since these quantities change with time, this effect needs to be accounted for accurate diagnosis. Additionally, to improve accuracy, the authors used the algorithm of ref. [10] to ensure there pressure from the arm does not cause a phase misalignment problem. Currently, the imaging is performed with a raster scanning stage hence image acquisition is on the order of minutes. As well as causing occlusion to the skin (the last point of which to be imaged will have been occluded for the longest), such acquisition times require the patient to be still for too long.

4. Fast THz modulation and image acquisition

Improved acquisition speed is greatly desired. Whilst there exist THz imaging arrays, they are narrow band and make hyperspectral studies impossible. Ideally one needs a fast way of efficiently modulating THz over a broadband range. Semiconductors such as high-resistivity silicon have plasma frequencies below the THz regime, however upon optical excitation the increase in charge carriers can move the plasma frequency above the THz regime [30, 31]. Therefore, by controlling the conductivity of semiconductors one can modulate THz over a broadband range with very high modulation depths. This idea has been used for THz imaging [17, 32]. Whilst the authors of ref.

[17] achieved ~95% amplitude modulation, they used a regenerative amplified laser system with fluences of ~100uJ/cm^2. As well as being expensive and big, the low-repetition rate of their laser system results in slow acquisition rates preventing real-world applicability. The need for such high optical powers is necessitated by performing their modulation in a transmission geometry. As demonstrated by Liu *et al* in ref. [22], one can achieve great modulation depth using lower optical excitation powers if the modulation is performed in a reflection geometry. Furthermore, the optimum signal to noise ratio is obtained when the THz beam is totally internally reflected from the semiconductor-air interface as this gives great modulation and also maximizes the detected signal. A similar modulation depth as ref. [17] is achieved despite using a low-cost, high-power LED as the optical pump compared to a regenerative amplified laser system used in ref. [17]. This is because in this total-internal-reflection (TIR) geometry, THz is much more sensitive to the conductive interface. This has also allowed Liu *et al* to achieve 99% THz modulation from one graphene layer [23].

The next step towards making cheap THz imagers is to incorporate some form of spatial patterning of the THz beam. In the optical pump approach, one can use a visible light spatial modulator. Since the optical pump is patterned, so are the conductive regions in the silicon and hence once imparts a spatial pattern on the THz beam. Measuring the resultant THz signal for many different spatial encoding masks allows a THz image via post-processing to be obtained [17, 33]. Most importantly, this method of imaging is compatible with single-element detectors, which are the most common type of THz detectors that offer hyperspectral capabilities. Additionally, one can reduce the acquisition times by performing image under-sampling techniques, such as adaptive-sampling [20, 34] and compressed sensing [18, 35], and also adaptively sample the THz pulse in the time-domain for further improvements [16]. However, the combination of all these methods in a single-works is yet to be accomplished.

5. Conclusions

Terahertz is highly sensitive to water concentrations, and since abnormal water content is very often associated with diseases, THz has great potential for uses in medical diagnosis. However, this great sensitivity comes with a price; the THz penetration depth is limited to around $100\,\mu m$ in most biological matter. This means non-invasive *in-vivo* measurements can only be performed on skin. Regardless, this has potential in the diagnosis of diabetic foot syndrome [3], in the monitoring of scar-healing processes [2] and in the determination of skin hydration levels [1, 4]. For these purposes, one needs to perform hyperspectral imaging and then process the data accurately. Extracting the THz properties of a sample in a consistent manner requires a reliable reference, and for this various calibration algorithms have been developed [9, 10], as outlined in section 2. After a calibration measurement over the entire imaging field of view, these techniques allow one to obtain the relevant reference signals from a single-measurement whilst taking into account imaging

window thickness variations, laser power fluctuations and the day-to-day performance of THz devices. To speed up the image acquisition speed fast, efficient and broadband THz modulators are being developed [22, 23]. The current approach is to perform the modulation in a reflection geometry as this increases the sensitivity to changes in the material conductance. With the development of such devices, THz technology is a step closer to being used in more clinical trials and commercially.

Acknowledgements

This work was partially supported by the Research Grants Council of Hong Kong (project numbers 14206717 and 14201415), the Hong Kong Innovation and Technology Fund (project number ITS/371/16), the Royal Society Wolfson Merit Award (EM) and the Hong Kong PhD Fellowship Award (QS).

References

[1] Z. D. Taylor et al.. "THz medical imaging: In vivo hydration sensing". *IEEE Trans. Terahertz Sci. Technol.*, 1, 1, 201–219 (2011).

[2] S. Fan, B. S. Y. Ung, E. P. J. Parrott, et al.. "In vivo terahertz reflection imaging of human scars during and after the healing process". *J. Biophotonics*, 10, 9, 1143–1151 (2017).

[3] G. G. Hernandez-Cardoso et al.. "Terahertz imaging for early screening of diabetic foot syndrome: A proof of concept". *Sci. Rep.*, 7, 42124, Feb (2017).

[4] Z. D. Taylor et al.. "THz and mm-wave sensing of corneal tissue water content: In vivo sensing and imaging results". *IEEE Trans. Terahertz Sci. Technol.*, 5, 2, 184-196 (2015).

[5] I. Ozheredov et al.. "In vivo THz sensing of the cornea of the eye". *Laser Phys. Lett.*, 15, 5, 55601, May (2018).

[6] N. Bajwa et al.. "Terahertz Imaging of Cutaneous Edema: Correlation with Magnetic Resonance Imaging in Burn Wounds". *IEEE Trans. Biomed. Eng.*, 64, 11, 2682-2694 (2017).

[7] K. I. Zaytsev, K. G. Kudrin, V. E. Karasik, et al.. "In vivo terahertz spectroscopy of pigmentary skin nevi: Pilot study of non-invasive early diagnosis of dysplasia". *Appl. Phys. Lett.*, 106, 5 (2015).

[8] R. I. Stantchev, J. C. Mansfield, R. S. Edginton, et al.. "Subwavelength hyperspectral THz studies of articular cartilage". *Sci. Rep.*, 8, 1, 6924, May (2018).

[9] S. Fan, E. P. J. Parrott, B. S. Y. Ung, et al.. "Calibration method to improve the accuracy of THz imaging and spectroscopy in reflection geometry". *Photonics Res.*, 4, 3, A29--A35, Jun (2016).

[10] X. Chen, E. P. J. Parrott, B. S. Y. Ung, et al.. "A Robust Baseline and Reference Modification and Acquisition Algorithm for Accurate THz Imaging". *IEEE Trans. Terahertz Sci. Technol.*, 7, 5, 493-501 (2017).

[11] K. I. Zaytsev, A. A. Gavdush, N. V. Chernomyrdin, et al. "Highly Accurate in Vivo Terahertz Spectroscopy of Healthy Skin: Variation of Refractive Index and Absorption Coefficient Along the Human Body". *IEEE Trans. Terahertz Sci. Technol.*, 5, 5, 817–827 (2015).

[12] S. Huang et al.. "Improved sample characterization in terahertz reflection imaging and spectroscopy". *Opt. Express*, 17, 5, 3848 (2009).

[13] Q. Sun, E. P. J. Parrott, Y. He, et al. "In vivo THz imaging of human skin: Accounting for occlusion effects". *J. Biophotonics*, 11, 2, e201700111, Feb (2018).

[14] Q. Sun et al.. "*In vivo* estimation of water diffusivity in occluded human skin using terahertz reflection spectroscopy". *J. Biophotonics*, e201800145, Jul (2018).

[15] P. Clarys, R. Clijsen, and A. O. Barel. "Influence of probe application pressure on in vitro and in vivo capacitance (Corneometer CM 825®) and conductance (Skicon 200 EX®) measurements". *Ski. Res. Technol.*, 17, 4, 445-450, Nov (2011).

[16] Y. He, E. P. J. Parrott, and E. Pickwell-MacPherson. "Adaptive Sampling for Terahertz Time-Domain Spectroscopy and Imaging". *IEEE Trans. Terahertz Sci. Technol.*, 7, 2, 118-123, Mar (2017).

[17] R. I. Stantchev et al.. "Noninvasive, near-field terahertz imaging of hidden objects using a single-pixel detector". *Sci. Adv.*, 2, 6, e1600190 (2016).

[18] C. M. Watts et al.. "Terahertz compressive imaging with metamaterial spatial light modulators". *Nat. Photonics*, 8, 8, 605-609 (2014).

[19] D. Shrekenhamer, C. M. Watts, and W. J. Padilla. "Terahertz single pixel imaging with an optically controlled dynamic spatial light modulator". *Opt. Express*, 21, 10, 12507 (2013).

[20] R. I. Stantchev, D. B. Phillips, P. Hobson, et al.. "Compressed sensing with near-field THz radiation". *Optica*, 4, 8, 989 (2017).

[21] T. Vasile, V. Damian, D. Coltuc, et al.. "Single pixel sensing for THz laser beam profiler based on Hadamard Transform". *Opt. Laser Technol.*, 79, 173-178 (2016).

[22] X. Liu, E. P. J. Parrott, B. S.-Y. Ung, et al.. "Exploiting total internal reflection geometry for efficient optical modulation of terahertz light". *APL Photonics*, 1, 7, 76103 (2016).

[23] X. Liu, Z. Chen, E. P. J. Parrott, et al.. "Graphene Based Terahertz Light Modulator in Total Internal Reflection Geometry". *Adv. Opt. Mater.*, 5, 3 (2017).

[24] R. Ulbricht, E. Hendry, J. Shan, et al.. "Carrier dynamics in semiconductors studied with time-resolved terahertz spectroscopy". *Rev. Mod. Phys.*, 83, 2, 543-586 (2011).

[25] H. Yada, M. Nagai, and K. Tanaka. "Origin of the fast relaxation component of water and heavy water revealed

by terahertz time-domain attenuated total reflection spectroscopy". *Chem. Phys. Lett.*, 464, 4, 166-170 (2008).

[26] J.-H. Son. *Terahertz biomedical science and technology*. Boca Raton: CRC Press, ch. 7.

[27] L. Thrane, R. H. Jacobsen, P. Uhd Jepsen, et al.. "THz reflection spectroscopy of liquid water". *Chem. Phys. Lett.*, 240, 4, 330-333 (1995).

[28] T. L. Tuan and L. S. Nichter. "The molecular basis of keloid and hypertrophic scar formation.". *Mol. Med. Today*, 4, January, 19-24 (1998).

[29] J. W. Lee et al.. "Terahertz spectroscopy of human sclera". *Curr. Appl. Phys.*, 15, 1156-1159 (2015).

[30] H. Alius and G. Dodel. "Amplitude-, phase-, and frequency modulation of far-infrared radiation by optical excitation of silicon". *Infrared Phys.*, 32, 1-11 (1991).

[31] A. Kannegulla, M. I. Bin Shams, L. Liu, et al.. "Photo-induced spatial modulation of THz waves: opportunities and limitations". *Opt. Express*, 23, 25, 32098 (2015).

[32] D. Shrekenhamer, C. M. Watts, and W. J. Padilla. "Terahertz single pixel imaging with an optically controlled dynamic spatial light modulator". *Opt. Express*, 21, 10, 12507, May (2013).

[33] B. Sun et al.. "3D computational imaging with single-pixel detectors". *Science (80-.).*, 340, 6134, 844-847 (2013).

[34] M. Amann and M. Bayer. "Compressive adaptive computational ghost imaging". *Sci. Rep.*, 3 (2013).

[35] Y. C. Eldar and G. Kutyniok. *Compressed sensing : theory and applications*. Cambridge University Press (2012).